JOURNAL OF SOLID STATE CHEMISTRY 117, 64–72 (1995)

Thermal Behavior and Magnetic Properties of Acicular Copper–Cobalt Ferrite Particles

Carole Villette, Philippe Tailhades, and Abel Rousset

Laboratoire de Chimie des Matériaux Inorganiques, URA CNRS 1311, Université Paul Sabatier, 118 route de Narbonne, 31062 Toulouse Cedex, France

Received December 10, 1994; accepted December 14, 1994

$Co_xCu_{1-x}Fe_2O_4$ ($0 \leq x < 0.3$) ferrite particles were prepared by a soft chemistry method using oxalic precursors. The ferrite particles obtained by this process are acicular in shape ($4.2 \leq L/D \leq 4.6$) ranging in length between 1.5 and 0.8 μm for $0 \leq x \leq 0.3$. Two series of samples were investigated: a first sample (SC) grouped together the ferrites slowly cooled from 710°C, and the second (Q) consisted of samples quenched from the same temperature. In contrast to the stability of the SC ferrites, the Q ferrites are subjected to two phenomena before reaching 400°C. The first is ascribed to the migration of Cu^{2+} ions from tetrahedral to octahedral sites. The second is the oxidation of Cu^{+} ions formed above 600°C during the preparation process and frozen by quenching at room temperature in the Q samples. Above approximately 400°C, no differences appear to subsist between SC and Q samples. They are both subjected to diffusionless order–disorder transformation, due to the modified orientation of the Jahn-Teller distorsions, and to the migration of Cu^{2+} ions from octahedral to tetrahedral sites, before the Curie temperature is reached. Magnetic measurements performed on the samples prepared for the present work reveal remarkably high and stable coercivities. These magnetic properties are due not only to the structural anisotropy, but also to the morphological characteristics. Because of their high and stable coercivities, submicron copper ferrites could be interesting pigments for magnetic recording.

INTRODUCTION

Copper ferrite ($CuFe_2O_4$) occurs, in different temperature domains, in two allotropic varieties, a tetragonally distorted spinel form which is stable at room temperature and a cubic spinel form which is stable at higher temperature (>350–400°C).

Cupric ions, when placed in octahedral sites ($CuFe_2O_4$) or tetrahedral sites ($CuCr_2O_4$), are recognized to be responsible for spinel lattice distortions, such as $c/a > 1$ (e.g., $CuFe_2O_4$) and $c/a < 1$ (e.g., $CuCr_2O_4$). These distorsions are caused by a cooperative Jahn-Teller effect related to the orientation of the distorted octahedra or tetrahedra in the same direction.

Various authors (1–3) suggest that the tetragonal–cubic transition results from the change in local deformations from an ordered arrangement to a random organization. This kind of transition is called diffusionless order–disorder transformation.

Ohnishi and Teranishi (4) and Bergstein and Cervinka (5) considered the influence of intersite cationic migration on the transformations. As shown by Néel (6) and Ohnishi and Teranishi (4), cupric ions can be displaced easily from one type of site to another by thermal treatments. Another proof of cationic migration is the thermal dependence of copper ferrite magnetization (6, 7). Samples quenched from different temperatures can thus be stabilized with varying tetragonal deformations. According to calculations by Finch *et al.* (2), the tetragonal deformation of $CuFe_2O_4$ only occurs when at least 33% of the octahedral sites are occupied by Cu^{2+} ions (i.e., at least 0.66 octahedral Cu^{2+} ions per formula unit). This critical content is 40% for Ohnishi *et al.* (8) and Tang.*et al.* (9). Besides the cupric ions location, the reduction of Cu^{2+} in Cu^{+} ions which occurs above around 600°C, appears to affect the tetragonal deformation amplitude (10).

The temperatures of order–disorder transformation depend on the content of octahedral cupric ions and on the nonstoichiometry (3, 4). Slowly cooled samples prepared by standard solid–solid reactions exhibit an order–disorder transformation at 360°C (8, 11). Weil *et al.* (12) and Ohnishi and Teranishi (4) found a tetragonal–cubic transformation at 760°C. This in fact corresponds to the lower quenching temperature required to stabilize the cubic structure at room temperature, but is unrelated to order–disorder transformation.

Copper ferrites display different thermal behavior before reaching 600°C, according to their tetragonal deformation amplitude (i.e., thermal history). Calorimetric measurements reveal two endothermic peaks at 390 and 490°C, when a slowly cooled sample is heated in air. These two peaks are ascribed to the Jahn-Teller transformation and the Curie temperature respectively (9). For a sample quenched from 550°C, two other exothermic

0022-4596/95 $6.00

peaks are observed at around 200 and 350°C. These are linked to Cu^{2+} ions migration from tetrahedral to octahedral sites, and to the oxidation of Cu^{+} ions respectively (9).

To sum up, the spinel lattice symmetry of $CuFe_2O_4$ can be modified by two main phenomena:

— diffusionless order–disorder transformation associated with disorientation of the Jahn-Teller distortions, and

— cationic migration and redox reactions which can alter the lattice symmetry especially through the cupric ion content in octahedral sites.

The first phenomenon transforms the tetragonally distorted spinel structure into a cubic lattice. It occurs at a temperature close to 360°C. The resulting cubic lattice cannot be stabilized at room temperature by quenching. On the other hand, the second phenomenon serves to obtain spinels with different c/a ratios by quenching samples from different temperatures. The cubic structure seems to be obtained for samples quenching from 760°C.

In contrast to the previous work, we prepared $Co_xCu_{1-x}Fe_2O_4$ ($0 \leq x < 0.3$) samples by a soft chemistry method, which enabled us to obtain acicular particles in a narrow grain size class. This paper presents the thermal study of the copper–cobalt ferrites prepared and annealed under different conditions. Changes in magnetic properties were also studied as a function of the structural characteristics and composition of the samples.

ANALYTICAL METHODS

The morphology of the powders was determined by scanning electron microscopy (SEM), using a JEOL JSM 6400. All the samples were analyzed by X ray diffraction using a Siemens X ray diffraction unit (model D501) and a cobalt target. This technique was used to determine sample purity, crystallite sizes using the Scherrer method, and the lattice constants. The latter were determined using rock salt (NaCl) as internal reference.

Differential scanning calorimetry (DSC) experiments were carried out under air or nitrogen with a SETARAM DSC 111G. Base line correction was not possible due to the reversibility of the phenomenon. These measurements were taken with about 65 mg of powder.

Thermal expansion under air flow was analyzed with a NETZSCH 402 E dilatometer. The powders were pressed (20×10^5 Pa) without binder into pellets 6 mm in diameter and about 3 mm thick.

Thermogravimetric analyses (TGA) were carried out under air flow with a SETARAM TAG 24 symmetric microbalance. Magnetization change (Curie temperature) was determined using a NETZSCH 409E thermobalance under magnetic field. If powder magnetization decreases with rising temperature, sample mass increases because the sample is less attracted by the magnetic field. Conversely, if sample magnetization increases, the mass drops.

Magnetic properties were measured on a S2IS pulsed-field magnetometer, which allows the application of a maximum magnetic field of 25 kOe.

EXPERIMENTAL RESULTS

Samples Preparation

$CuFe_2O_4$ and $Co_xCu_{1-x}Fe_2O_4$ particles were prepared by a "chimie douce" method using oxalic precursors. This method consists of two main stages. In the first, a concentrated solution of cupric, cobaltous, and ferrous chlorides is precipitated at room temperature, in an oxalic acid solution. The metallic salts are dissolved in a mixture of water, ethylene glycol, and hydrochloric acid. The oxalic acid is dissolved in ethyl alcohol (95%) and water (5%). These alcoholic solutions, for which the dielectric constants are sharply lower than those for water, usually help obtain oxalate particles smaller than those in aqueous medium alone (13). Moreover, in pure water, we observed that the chemical precipitation of copper and iron ions by oxalic acid leads to the formation of the α-$FeC_2O_4 \cdot 2H_2O$ (14) (or α-$(Fe_{1-y}Co_y)C_2O_4 \cdot 2H_2O$) allotropic variety and $CuC_2O_4 \cdot H_2O$, in agreement with previous results (15). On the other hand, in the alcoholic medium previously described, a pure mixed oxalate is obtained, despite the structural differences between iron and copper oxalates (16).

In fact, the X ray diffraction patterns of the oxalate prepared reveal only one system of lines, which is similar to the X ray diagram of β-$FeC_2O_4 \cdot 2H_2O$ described by Deyrieux and Peneloux (14). Evidence of the substitution of iron by copper is provided by the modification of the lattice constants. For example, these become $a = 1.206$ nm, $b = 0.547$ nm, $c = 1.566$ nm for a mixed oxalate Cu : Fe = 1 : 2, instead of $a = 1.226$ nm, $b = 0.557$ nm, $c = 1.548$ for β-$FeC_2O_4 \cdot 2H_2O$ (14). The weight loss found by thermogravimetric measurements also shows good agreement for the mixed oxalates, with a general formula like $Cu_{(1-x)/3}Co_{x/3}Fe_{2/3}C_2O_4 \cdot 2H_2O$.

In the second stage, the oxalic precursors are slowly decomposed under air flow, treated at 710°C for 4 hr and quenched (Q samples) or slowly cooled at −10°C/hr (SC samples). The resulting products are single tetragonal or cubic spinel phases (Table 1). The heat treatment used allows the pseudomorphic transformation of the acicular oxalate crystals, leading to acicular ferrite particles (Fig. 1). Depending on the composition the average length and acicular ratio of the particles are contained between 1.5 and 0.8 μm and 4.6 and 4.2 respectively for $0 \leq x \leq 0.3$.

TABLE 1
Morphological and Structure Deformation Versus Cobalt Content

x	Particle length, L (μ)	Particle diameter, D (μ)	L/D	Slowly cooled c/a	Quenched c/a
0	1.5	0.33	4.6	1.06	1.047
0.07	1.2	0.3	4.5	1.053	1.032
0.15	1.1	0.25	4.4	1.043	1.0
0.2	1.0	0.25	4.4	1.037	1.0
0.33	0.8	0.2	4.2	1.0	1.0
0.44	0.4	0.13	3.7	1.0	1.0

The average crystallite size measured from X ray line broadening was close to 45 nm.

Thermal Behavior of Slowly Cooled Samples

The thermal behavior under air of the SC $CuFe_2O_4$ samples was studied by several techniques. On heating (10°C/min) calorimetric analyses indicate two endothermic peaks A and B, which become exothermic on cooling (Fig. 2).

The first phenomenon (A peaks) occurs at lower temperature and decreases in amplitude, when a part of the copper ions is substituted by cobalt ions (Fig. 3). This can be attributed to the transition from ordered to randomly oriented Jahn-Teller distortions. This tetragonal/cubic transition becomes easier and less extensive if the octahedral Cu^{2+} ions are replaced by cobalt ions. Moreover, the disorder of the orientations of Jahn-Teller distortions cannot be frozen at room temperature by quenching the samples, after annealing in the temperature range in which the A phenomena occurs.

The second phenomenon (B peaks) occurs at a temperature that varies slightly with the copper content (Fig. 3). For the compositions studied here, the B peaks are observed in the range 490–500°C, close to the Curie temperature of $CuFe_2O_4$ (11). Moreover, under the previous experimental conditions, calorimetric analysis on $CoFe_2O_4$ highlights a peak at 516°C, which fits well with the Curie point reported for this compound (17).

Two kinds of phenomena are revealed by dilatometry (Fig. 4) corresponding to increases in sample volume. The first (A' peaks), which appears in the same temperature range as the previous A peaks, is also ascribed to the reorientation of the Jahn-Teller distortions. The second (C') is observed at a constant temperature (450°C) lower than that for the calorimetric B peaks. To interpret the C' peaks, all the SC samples were subjected to successive annealings for 2 hr at increasing temperatures. The samples were quenched after each annealing, and their c/a ratios were measured at room temperature (Fig. 5). A drop in the c/a ratio is observed in the same temperature range (400–600°C) irrespective of the copper content. This suggests that the C' peaks are also correlated with the decrease in the c/a ratio. More precisely, from bibliographic data (4), the migration of Cu^{2+} ions from octahe-

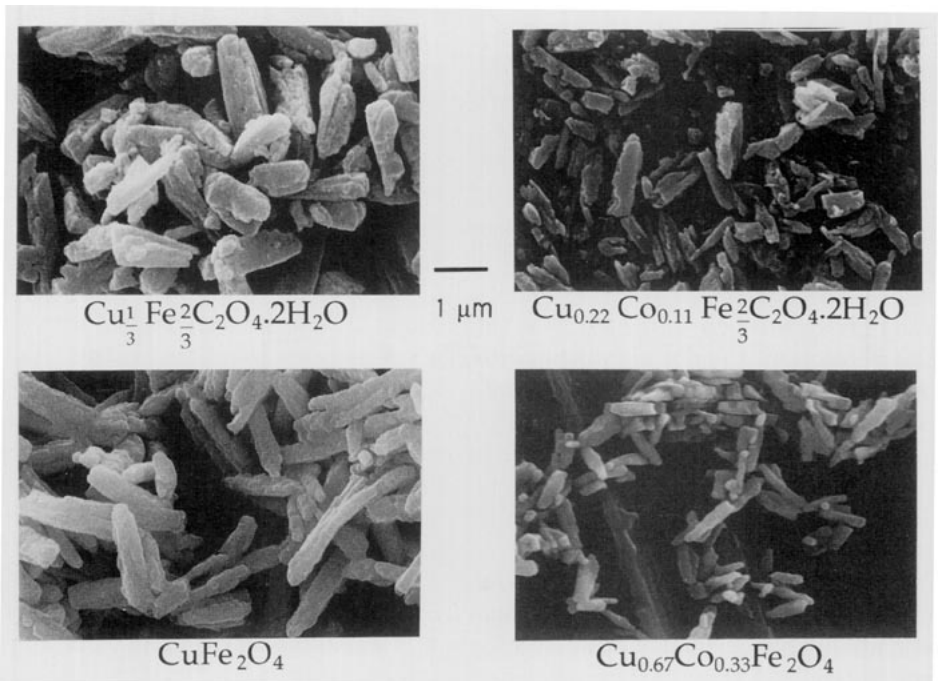

FIG. 1. Electron micrograph of $Cu_{(1-x)/3}Co_{(x/3)}Fe_{2/3}C_2O_4 \cdot 2H_2O$ particles and $Cu_{(1-x)}Co_xFe_2O_4$ particles prepared from oxalic precursor.

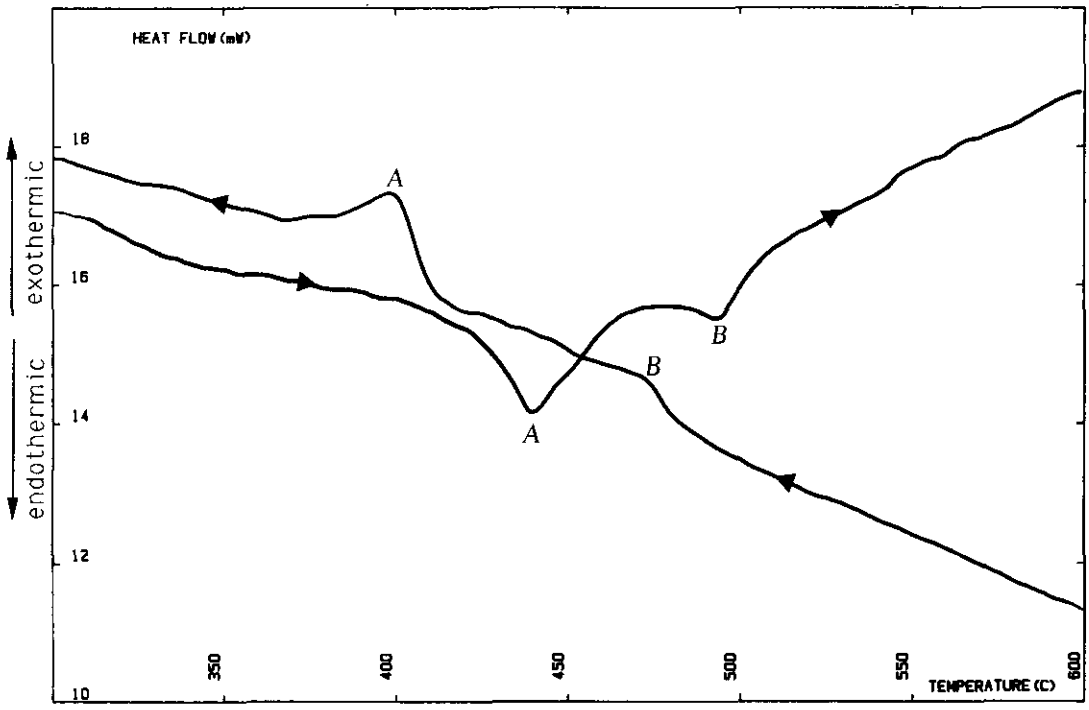

FIG. 2. Differential scanning calorimetry (DSC) curves for slowly cooled (SC) copper ferrite $CuFe_2O_4$, heating rate ±10°C/min.

dral to tetrahedral sites is responsible for this decrease. Hence the C' peaks reveal these migrations.

For $CuFe_2O_4$, thermogravimetric analysis under a low magnetic field reveals two apparent variations in mass corresponding to modifications of the magnetic properties due to the Jahn-Teller transitions (A'' shifts in Fig. 6)

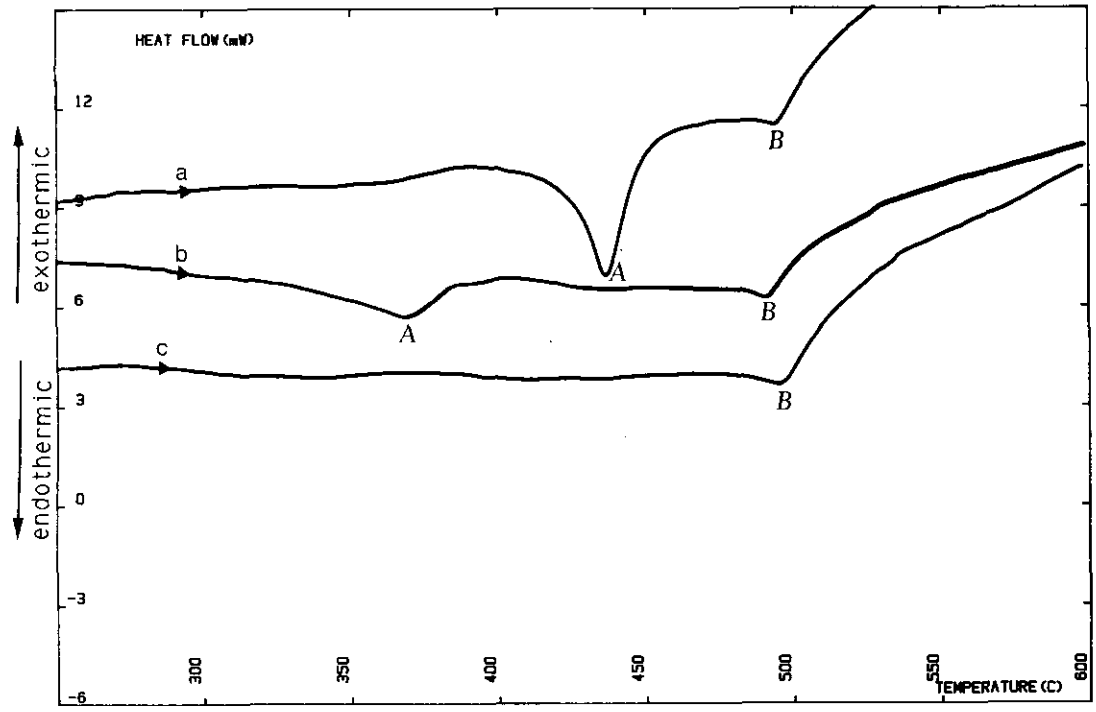

FIG. 3. DSC curves for slowly cooled $Cu_{1-x}Co_xFe_2O_4$, heating rate 10°C/min: (a) $CuFe_2O_4$, (b) $Cu_{0.93}Co_{0.07}Fe_2O_4$, (c) $Cu_{0.66}Co_{0.34}Fe_2O_4$.

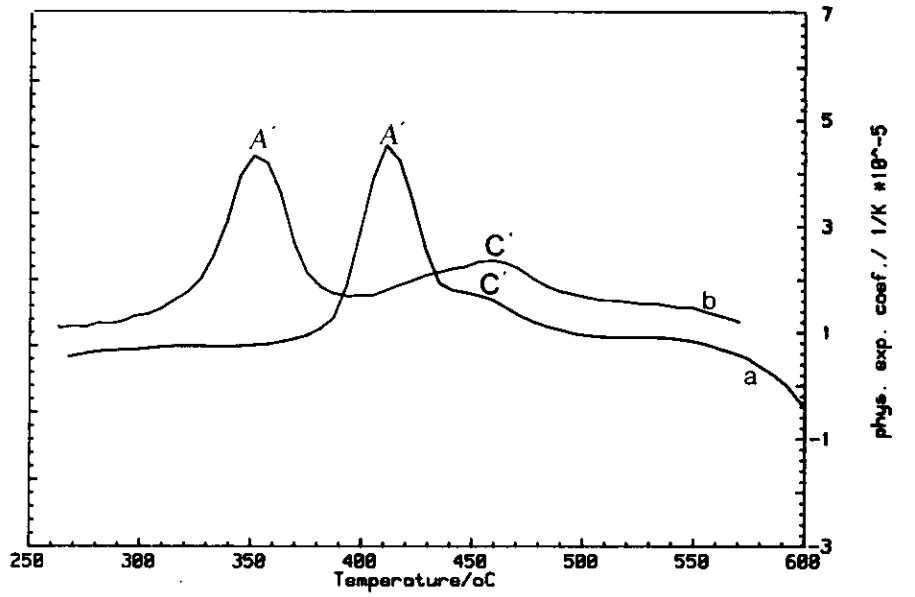

FIG. 4. Differential dilatometry curves for slowly cooled $Cu_{1-x}Co_xFe_2O_4$, heating rate 10°C/min: (a) $CuFe_2O_4$, (b) $Cu_{0.93}Co_{0.07}Fe_2O_4$.

and the Curie temperatures respectively (B'' shifts). The A'' variations in mass effectively occur at the same temperature as the A peaks on calorimetric curves, and their amplitude decreases with increasing cobalt content, because of the weak Jahn-Teller effects in Co–Cu ferrites. The B'' shifts appear also at temperatures close to those of the B peaks. However, thermomagnetic measurements reveal a slight increase in Curie temperature with cobalt content, which is consistent with the difference in the Curie points between $CuFe_2O_4$ (T_c = 490°C) and $CoFe_2O_4$ (T_c = 520°C).

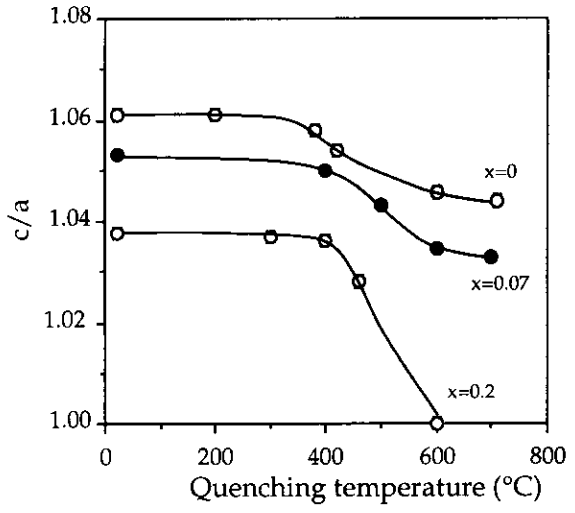

FIG. 5. Variation in c/a ratio versus temperature from which $Cu_{1-x}Co_xFe_2O_4$ was quenched.

Thermal Behavior of Quenched Samples

Calorimetric and dilatometric analyses (Figs. 7 and 8), carried out under the same conditions as previously show five phenomena for the quenched samples. At the highest temperatures (420–550°C) they display the same thermal behavior as the slowly cooled samples. Peaks A, B, and C' described above are again observed. Below 420°C, however two other peaks appear in the ranges 250–350°C (α peaks) and 350–420°C (β peaks).

Table 2 shows that the Q samples always have higher unit cell volumes and magnetizations than the SC samples. From bibliographic data, these differences are due to variations in cationic distributions and stoichiometries. It is generally acknowledged that samples

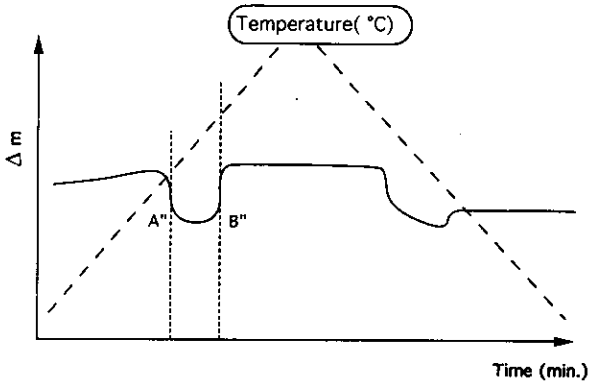

FIG. 6. Thermogravimetry curve of copper ferrite $CuFe_2O_4$ under magnetic field, heating rate 10°C/min.

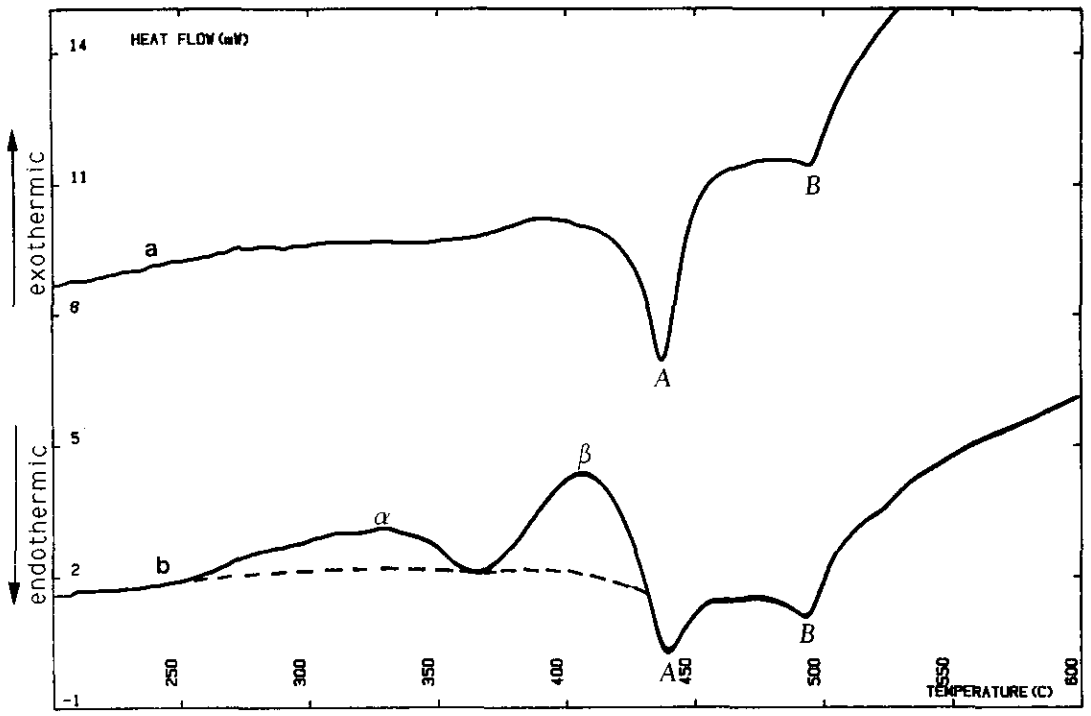

FIG. 7. DSC curves for quenched and slow cooled $CuFe_2O_4$, heating rate 10°C/min: (a) slowly cooled, (b) quenched.

quenched from temperatures higher than 600°C are oxygen deficient and have Cu^{2+} ions on both octahedral and tetrahedral sites, while SC samples are close to the stoichiometry and only have octahedral cupric ions. The α and β peaks seem to be related to these chemical and structural differences.

The phenomena at 250–350°C (α peaks) are revealed by exothermic peaks for the calorimetric curves and by negative peaks (volume contractions) for the dilatometric curves. These peaks keep the same profile when the analyses are carried out in an inert atmosphere (N_2), which rules out ascribing the peaks to any oxidation reaction. In

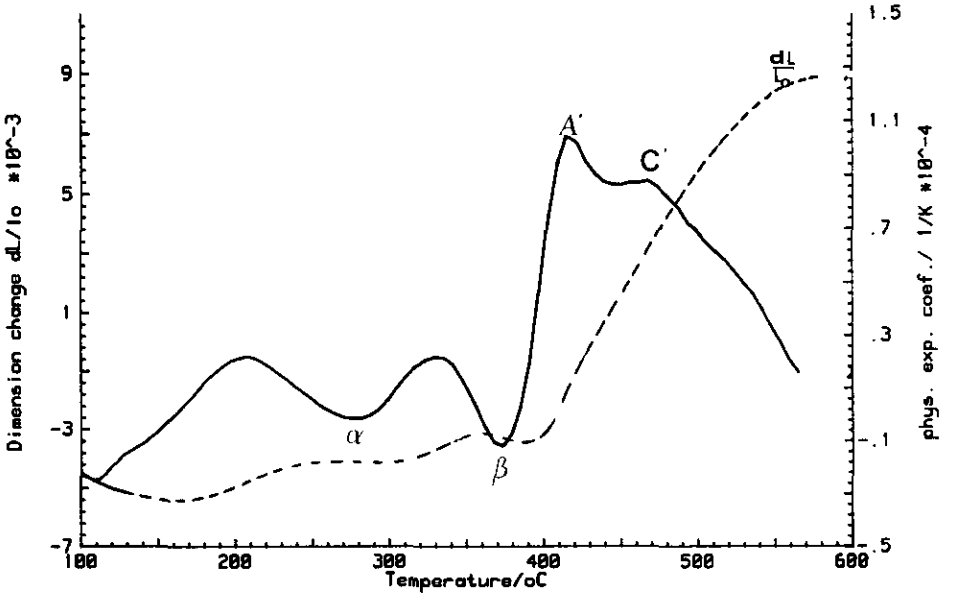

FIG. 8. Dilatometry and differential dilatometry curves (measured by Netzsch Dilatometer 402 E) for quenched $CuFe_2O_4$, heating rate 10°C/min.

TABLE 2
Unit Cell Volume and Magnetization Versus Cobalt Content

	Slowly cooled		Quenched	
x	Unit cell volume 10^{-22} (cm^3)	Saturation magnetization (20°C) (emu/g)	Unit cell volume 10^{-22} (cm^3)	Saturation magnetization (20°C) (emu/g)
0	5.88	25.0	5.89	38.0
0.07	5.88	25.8	5.89	46.8
0.15	5.87	28.9	5.88	43.0
0.2	5.88	31.4	5.88	41.5
0.33	5.87	41.8	5.89	55.4
0.44	5.87	49.2	5.89	56.2

contrast, the β exothermic peaks disappear when the analyses are carried out under nitrogen. Otherwise, above 420°C in order to observe A peaks with a similar amplitude as for the SC samples, it would be necessary for the Q samples to have approximately the same octahedral Cu^{2+} ion content at these temperatures, as if they were slowly cooled during preparation. This implies Cu^{2+} ions migrations from tetrahedral to octahedral sites below 420°C. The α peaks, which are independent of the treatment atmosphere, could then be ascribed to these cationic migrations.

This interpretation is consistent with the volume contraction observed in the range 250–350°C. The unit cell volumes of quenched samples are in fact higher than those for the slowly cooled samples, i.e., samples having only octahedral Cu^{2+} ions (Table. 2). Further proof of cupric ions migration from tetrahedral to octahedral sites is also provided by the measurements of the c/a ratios of Q samples annealed at increasing temperatures (Fig. 9). As it may be expected from the above interpretation, the tetragonal deformation becomes more marked from 150°C, as soon as the samples are annealed in air (or nitrogen). By contrast, this deformation tends to disappear, as for the SC samples, when the treatments are carried out above 400°C in air (no annealing was carried out in nitrogen above 350°C, because of the demixtion of the initial spinel phase into CuO, $CuFeO_2$, and a tetragonal spinel phase).

The β exothermic peaks, which disappear under nitrogen atmosphere, are ascribed to oxidation, particularly the oxidation of Cu^+ ions due to the nonstoichiometry mentioned above.

Oxidations corresponding to the β peaks can be also identified by thermogravimetric analysis using a slow heating rate (3°C/min.) to preserve a good base line (Fig. 10). According to the thermogravimetric results, less than 0.02 Cu^+ ions per formula unit are completely oxidized at 400°C. Under the same experimental conditions, a study of the reactivity of $Cu_xFe_{3-x}O_4$ powders, having the same crystallite size as the powders used here, show that the oxidation of Cu^+ ions in the octahedral or tetrahedral sites of the spinel structure occurs below 300°C (18). This difference in reactivity could be ascribed to the presence of Cu^+ ions in "interstitial" sites, as suggested by Gleitzer and Goodenough (19).

Magnetic Properties

The coercivities of SC and Q samples obviously depend on the cobalt content (Fig. 11). Indeed the strong magnetocrystalline anisotropy of the octahedral Co^{2+} ions contributes to the strengthening of the coercive force. However the change in coercive force with cobalt content (x) results not only from the magnetocrystalline anisotropy of the Co^{2+} ions, but also the tetragonal deformation of the spinel lattice. The latter influence is obvious if we plot coercivity versus c/a ratio of SC samples annealed below 710°C and quenched from their annealing temperature (Fig. 12). The opposite variations of the influence of magnetocrystalline anisotropy increasing with x, and the structural anisotropy due to tetragonal deformation decreasing with x, leads to a maximum for x close to 0.2. This maximum is not observed for $H_c = f(x)$ curves of the cubic spinel solid solutions γ-Fe_2O_3–$CoFe_2O_4$, and $Co_xFe_{3-x}O_4$, (20, 21) for which a maximum is observed for x close to 0.7–0.8.

A comparison of the coercivities of the SC and Q $CuFe_2O_4$ samples with the bibliographic data (12, 15, 22) shows that the samples investigated have the highest coercive forces at room temperature. This suggests a con-

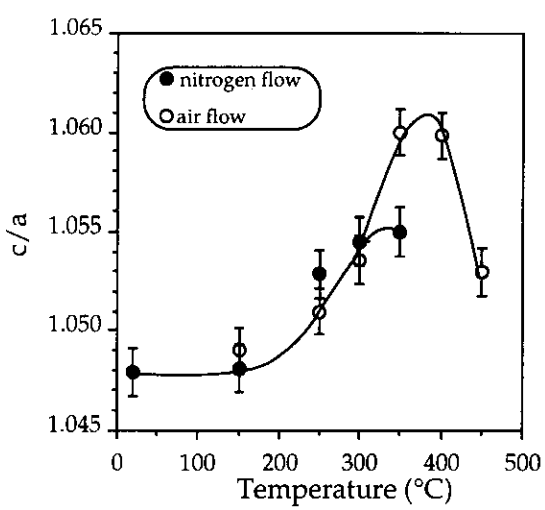

FIG. 9. Variation in tetragonal deformation (c/a) versus annealing temperature, under air or nitrogen flow, from which Q $CuFe_2O_4$ ferrite was quenched.

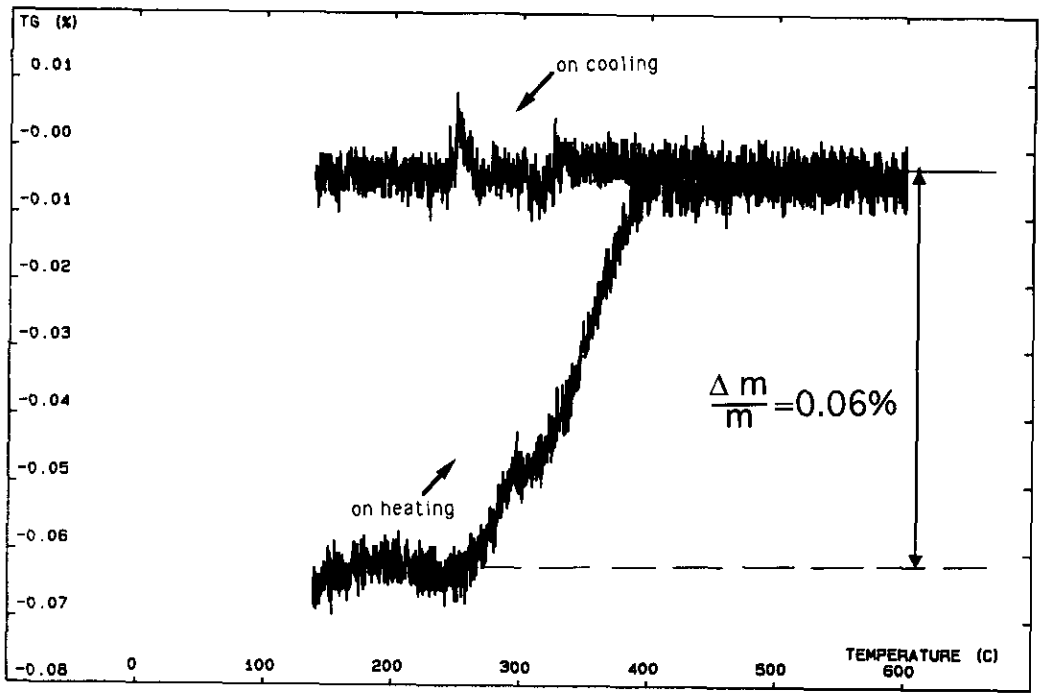

FIG. 10. Thermogravimetry (TGA) curve of quenched copper ferrite $CuFe_2O_4$ under air flow.

tribution of the morphological and granulometric characteristics of the particles (Fig. 1). They in fact display an acicular shape and small sizes, leading respectively to a strong shape anisotropy and probably to the behavior of single domain particles, in contrast to the samples studied thus far.

The combination of structural anisotropy with shape anisotropy gives very high coercivities (up to 1600 Oe) for the more tetragonally distorted $CuFe_2O_4$ particles, even when they are cobalt free (Fig. 12). $CuFe_2O_4$ samples also have coercivities with outstanding thermal stabilities, making copper ferrites highly interesting as magnetic recording materials. In fact, close to room temperature, the dH_c/dT coefficients corresponding to coercive forces of 730, 1170, and 1520 Oe are -0.7, -0.9, and -1.3 Oe/°C respectively. These thermal variations are less than 0.1%/°C if we consider the absolute value of $(dH_c/dT)/H_c$. This value is far lower than that for cobalt substituted ferrites (0.5 to 1%/°C) (23, 24) or for cobalt

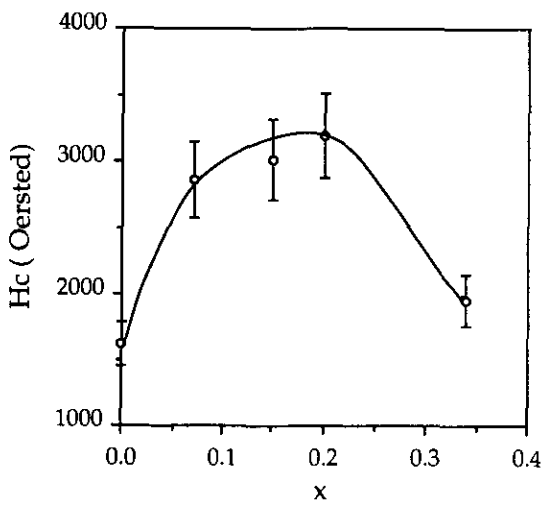

FIG. 11. Variation in coercive force (H_c) versus cobalt content.

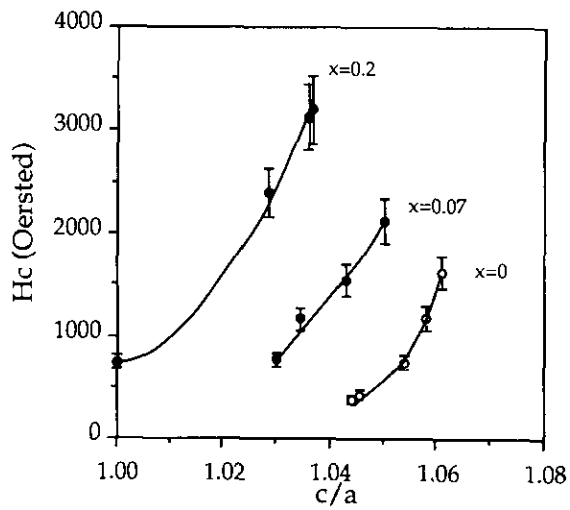

FIG. 12. Variation in coercive force (H_c) versus tetragonal deformation (c/a) of $Cu_{1-x}Co_xFe_2O_4$ unit cell.

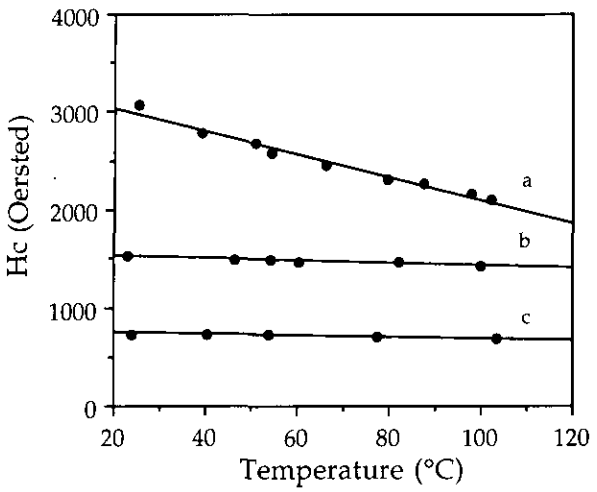

FIG. 13. Thermal dependence of coercivities (H_c) for $Cu_{1-x}Co_xFe_2O_4$ ferrite samples: (a) $Cu_{0.8}Co_{0.2}Fe_2O_4$, $c/a = 1.036$; (b) $CuFe_2O_4$, $c/a = 1.06$; (c) $CuFe_2O_4$, $c/a = 1.054$.

surface-doped ferrites (0.2 to 0.5%/°C) (24, 25), although these materials were specially developed for excellent thermal stability of coercivity.

However, the remanent magnetizations of the copper ferrites samples are low (10 to 15 emu/g) for magnetic recording applications and despite the fact that cobalt bulk doping increases the remanence (17 emu/g for $x = 0.2$), this property enhancement is offset by the lower thermal stability of coercivity (Fig. 13).

CONCLUSION

Mixed acicular and monodispersed $Cu_{(1-x)/3}Co_{x/3}Fe_{2/3}C_2O_4 \cdot 2H_2O$ particles were precipitated by making two alcoholic solutions react, one of metal salts and the second of oxalic acid. These oxalic precursors can be treated at moderate temperature (710°C) to yield $Co_xCu_{1-x}Fe_2O_4$ spinels. Slow decomposition under air flow up to 710°C allows pseudomorphic transformation of the oxalate particles to give small acicular ferrite particles with a narrow size distribution.

All the ferrite samples studied were prepared at the same temperature, but one series was slowly cooled from 710°C to room temperature, and another was quenched from 710°C. The SC and Q samples displayed different thermal behavior, which was interpreted as follows.

In contrast to the stability of SC ferrites, Q ferrites are subjected to two phenomena before reaching 400°C. The first is ascribed to the migration of Cu^{2+} ions from tetrahedral to octahedral sites. The second is the oxidation of Cu^+ ions formed above 600°C during the preparation process and frozen by quenching at room temperature in the Q samples. Above approximately 400°C, no difference appears to subsist between SC and Q samples. They are both subjected to diffusionless order–disorder transformation, due to the modified of the orientation of the Jahn-Teller distortions, and to the migration of Cu^{2+} ions, from octahedral to tetrahedral sites before the Curie temperature is reached.

These interpretations are consistent with the results of Tang *et al.* (9) obtained for $CuFe_2O_4$ prepared by a conventional ceramic method. However, magnetic measurements taken on the samples prepared for the present work revealed remarkably high and stable coercivities. These magnetic properties are due not only to the structural anisotropy, but also to the morphological characteristics. The samples obtained from oxalic precursors in fact display strong anisotropy shape and small grain size, distinguishing them from the copper ferrites prepared thus far.

Owing to their high and stable coercivities, submicron copper ferrites could be interesting pigments for magnetic recording. However, their low magnetization will have to be increased. Cobalt volume doping improves the remanent magnetization but causes excessive thermal dependence of coercivity. Other avenues for developing copper ferrites for high density magnetic recording need to be investigated.

REFERENCES

1. P. Wojtowicz, *Phys. Rev.* **116**(1), 32 (1959).
2. G. I. Finch, F. R. S. Sinha, and K. P. Sinha, *Proc. R. Soc. London Ser. A Math. Phys. Sci.* **242,** 28 (1957).
3. H. M. O'Bryan, H. J. Levinstein, and R. C. Sherwood, *J. Appl. Phys.* **37**(3), 1437 (1966).
4. H. Ohnishi and T. Teranishi, *J. Phys. Soc. Jpn.* **16**(1), 35 (1961).
5. A. Bergstein and L. Cervinka, *Czech. J. Phys. Ser. B* **11,** 584 (1961).
6. L. Néel, *C. R. Acad. Sci. Paris* 190 (1950).
7. R. Pauthenet and L. Bochirol, *J. Phys. Rad.* **12,** 249 (1951).
8. H. Ohnishi, T. Teranishi, and S. Miyahara, *J. Phys. Soc. Jpn.* **14,** 106 (1959).
9. X. X. Tang, A. Manthiram, and J. B. Goodenough, *J. Solid State Chem.* **79,** 250 (1989).
10. S. Sahara and T. Yamaguchi, *J. Appl. Phys.* **37,** 3324 (1966).
11. J. Mexmain, *Ann. Chim.* **4,** 429 (1969).
12. L. Weil, F. Bertaut, and L. Bochirol, *J. Phys. Rad.* **11,** 208 (1950).
13. Ph. Tailhades, thesis, Toulouse, 1988.
14. R. Deyrieux and A. Peneloux, *Bull. Soc. Chim. Fr.* 2675 (1969).
15. A. M. Berkowitz and W. J. Schuele, *J. Appl. Phys.* **30**(4), 134S (1959).
16. H. Fichtner-Schmittler, *Cryst. Res. Technol.* **19,** 1225 (1984).
17. E. P. Wohlfarth, "Ferromagnetic Materials." North-Holland, Netherlands, 1986.
18. To be published.
19. C. Gleitzer and B. Goodenough, "Structure and Bonding," Vol. 61. Springer–Verlag, Berlin, 1985.
20. N. N. Evtihiev, N. A. Economov, A. R. Krels, N. A. Zanijatina, V. D. Baurin, and V. G. Pinko, *IEEE Trans. Magn.* **12**(6), 773 (1976).
21. W. D. Haller, M. Colline, U.S. Patent 3,573,980 (191).
22. R. Forrer, R. Baffie, and P. Fournier, *J. Phys.* **3,** 71 (1945).
23. M. P. Sharrock, *IEEE Trans. Magn.* **25,** 4374 (1989).
24. Ph. Tailhades, Ch. Sarda, P. Mollard, and A. Rousset, *J. Magn. Magn. Mater.* **89,** 33 (1990).
25. M. Kishimoto, S. Kitaoka, H. Hando, M. Amemiya, and F. Hayama, *IEEE Trans. Magn.* **17**(6), 3029 (1981).